

Baryon asymmetry from electroweak tachyonic preheating

Anders Tranberg and Jan Smit

*Institute for Theoretical Physics, University of Amsterdam,
Valckenierstraat 65, 1018 XE Amsterdam, the Netherlands.*

ABSTRACT: We consider a scenario in which the baryon asymmetry was created in the early universe during a cold electroweak transition. The spinodal instability of the Higgs field caused by a rapid change of sign of its effective mass-squared parameter induces tachyonic preheating. We study the development of Chern-Simons number in this transition by numerical lattice simulations of the SU(2)-Higgs model with an added effective CP-violating term. A net asymmetry is produced, and we study its dependence on the size of CP violation and the ratio of Higgs to W mass.

KEYWORDS: Baryogenesis, CP violation, Out-of-equilibrium field theory, Preheating, Symmetry breaking.

Contents

1. Introduction	1
2. Tachyonic electroweak preheating	5
3. The SU(2)-Higgs model	7
4. Initial conditions and classical approximation	9
4.1 Just-the-half distribution	11
4.2 Thermal distribution	11
5. Numerical simulation	11
5.1 Observables	12
5.2 Single trajectories	12
5.3 Ensemble averages	15
5.4 Initial rise	17
5.5 Final temperature and sphaleron wash-out	19
5.6 Effective sphaleron rate	20
6. Conclusion	21
A. Lattice formulation	22
A.1 Action	23
A.2 Equations of motion	24
A.3 Chern-Simons number and winding number	25
B. Coping with the Gauss constraints	25
B.1 Initial Higgs fields	25
B.2 Initial gauge fields	27

1. Introduction

The baryon number asymmetry of the Universe, expressed in terms of the observed ratio of baryon number density (n_B) to photon number density (n_γ) [1]

$$\frac{n_B}{n_\gamma} = 6.5_{-0.3}^{+0.4} \times 10^{-10} \quad (1.1)$$

is thought to be the result of high energy processes in the very early Universe. These processes need to break charge conjugation symmetry (C), the symmetry under the combined

charge conjugation and parity (CP) and conservation of baryon number (B). In addition it is necessary for the processes to take place during a period when the Universe was sufficiently out of thermal equilibrium [2].

Quite a few theories of baryogenesis have been proposed that can explain the order of magnitude of the asymmetry (1.1), see e.g. the review [3]. Most of these are based on physics beyond the Standard Model (SM) and because of our limited knowledge of this physics and of the history of the very early universe, it is hard to falsify a particular proposal. We consider it therefore important to search for a viable scenario of baryogenesis within the known physics of the Standard Model. We should also include its renormalizable extension that includes right-handed neutrino fields and Dirac and Majorana mass terms — which we shall call the Extended Standard Model (ESM) — to incorporate the neutrino masses.

In the (E)SM all criteria for baryogenesis are met. Baryon number is violated through an anomaly [4] and the weak interactions violate C and CP. For three or more generations, CP violation in the quark sector is possible through the Cabibbo-Kobayashi-Maskawa (CKM) mixing matrix [5, 6]. Experimentally, three generations are observed and the measured CP violation in Kaon and heavy-quark systems is consistent with the CKM matrix [7]. There may be more sources of CP violation in the neutrino sector, thus far hidden in the neutrino mixing matrix. The required non-equilibrium may be found in the decay of heavy neutrinos falling out of thermal equilibrium at temperatures $T > 10^8$ GeV [8] — the leptogenesis scenario — or in the electroweak transition.

Tachyonic electroweak transition

It is a great challenge to develop a scheme in which the baryon asymmetry follows from the physics of the (E)SM at an energy scale of order 100 GeV. At this energy scale the Hubble rate is only about 10^{-5} eV and the required non-equilibrium dynamics is then to be caused by the electroweak transition. Such schemes fall under the unifying name of electroweak baryogenesis [9, 10, 11]. Most schemes rely on the electroweak transition being a sufficiently strong first-order finite-temperature phase transition. It was found later that the electroweak transition cannot be first order in the Standard Model [12, 13], given the experimental bound on the Higgs mass $m_H > 114$ GeV [7]. This has led to investigations of whether the phase transition can be first order in theories with an extended Higgs sector, such as the Minimal Supersymmetric Standard Model [14, 15].

Another possibility for the required out-of-equilibrium conditions is preheating at the electroweak scale after low-scale inflation, either through resonant preheating [16, 17], or tachyonic preheating and the creation of topological defects [17, 18]. In these scenarios the electroweak transition is not a regular finite-temperature transition but a *cold* transition, caused by a hybrid-inflation type coupling of the Higgs field to an inflaton field. Such electroweak transitions have been investigated in more detail [19, 20], and the tachyonic case appears most promising [21, 22, 23].

In such a tachyonic electroweak scenario for baryogenesis, the baryon number generated

during the transition is given by the anomaly equation

$$B(t) = 3\langle N_{\text{CS}}(t) - N_{\text{CS}}(0) \rangle, \quad (1.2)$$

where N_{CS} is the Chern-Simons number in the SU(2) gauge fields and B is assumed to be negligible (e.g. due to inflation) before the transition at time $t = 0$. A sufficient CP bias is needed to produce the observed asymmetry (1.1).

CP violation

A further hurdle to be overcome is the strength of CP violation. In the Standard Model this has been estimated as being of order [24]

$$J (y_u - y_c)^2 (y_c - y_t)^2 (y_t - y_u)^2 (y_d - y_s)^2 (y_s - y_b)^2 (y_b - y_d)^2 \approx 10^{-23}, \quad (1.3)$$

where y_u, \dots, y_t are the fermion-Higgs Yukawa couplings and [7]

$$J = |\text{Im}(V_{ij}V_{kl}V_{il}^*V_{kj}^*)| = (3 \pm 0.3) \times 10^{-5} \quad (1.4)$$

is the simplest rephasing-invariant combination of the CKM matrix V . In [25, 26, 10] finite-temperature estimates were given with $y_f \rightarrow m_f^2/T^2$ and T of order of the electroweak transition, $T \approx 100$ GeV, which led to a magnitude $\approx 10^{-20}$. Clearly, if these estimates are to be taken seriously, Standard Model CP-violation is much too weak for baryogenesis, which is the current lore.

CP violation is a subtle effect based on quantum mechanical interference, which can be destroyed at high temperatures. The above finite-temperature estimate can perhaps be justified by a high-temperature expansion and dimensional reasoning. However, the zero temperature estimate (1.3) seems less reliable to us, since it contradicts the measured magnitude of CP-violating observables. Factors such as J are hard to avoid in analytical calculations, but the product of Yukawa couplings in (1.3) could be compensated by perturbative energy-denominators or non-perturbative effects (see e.g. [27, 28, 29] and [30]). We found indications of such compensation in a computation of the effective action obtained by integrating out the fermions [31].

One motivation for our work here is the possibility that *at zero temperature* the strength of CP violation in the SM is given by J , i.e. without the product of y 's. This is another reason for considering scenarios based on a tachyonic electroweak transition. In the ESM with Majorana masses there is less rephasing-invariance and the corresponding $J' = \text{Im}(V'_{ij}V'_{ik}^*)$ could be even larger.

Sphaleron transitions

It is important that the effective temperature after the transition is low enough for sphaleron processes to be strongly suppressed, otherwise B might diffuse to zero again (see [32, 33] for recent results on the magnitude of the sphaleron rate). Because a tachyonic transition occurs at a relatively low energy, which becomes redistributed over the many degrees of freedom by the efficiency of the preheating process, sphaleron wash-out is not expected to

be a problem, as already suggested in [16]. A recent study [34] of Higgs- and W-particle numbers shortly after a tachyonic electroweak transition indeed showed low effective temperatures. However, particle numbers in the important low momentum modes were found to be still rather large, corresponding to large chemical potentials [34], suggesting the possibility of a sizable effective sphaleron rate after the transition.

This work

In this paper we report on a study of the asymmetry generated in a tachyonic electroweak transition by lattice simulations of the SU(2)-Higgs model with effective CP violation. The transition is modelled by a rapid quench and we use a classical approximation that can be justified for such transitions [21, 22]; the quantum average is approximated by an average over a classical ensemble of initial conditions, which is evolved using classical equations of motion.

The effective CP violation we use is given by a term

$$\kappa \phi^\dagger \phi \text{Tr} [F^{\mu\nu} \tilde{F}_{\mu\nu}] \quad (1.5)$$

in the lagrangian (ϕ is the Higgs doublet, $F^{\mu\nu}$ the gauge field strength tensor and $\tilde{F}_{\mu\nu}$ its dual). The coefficient κ parametrizes the CP violation and has mass dimension -2 . One may write it as

$$\kappa = \frac{3\delta_{CP}}{16\pi^2 M^2} \quad (1.6)$$

where M is some mass scale and δ_{CP} is dimensionless.

There are two possible interpretations of the term (1.5). We can see it as a crude representation of the CP violation due to the fermions in the (E)SM, in which case we choose $M = m_W$. In the second interpretation the term (1.5) could be the lowest-dimensional CP-violating operator resulting from integrating out heavy fermions (with masses beyond the electroweak scale) in a path integral, in a large class of theories beyond the Standard Model. In this case we choose $M = 1$ TeV. Notwithstanding the approximate nature of the model, which neglects the dynamics of the (E)SM fermions as well as the U(1) and SU(3) gauge fields, it is very interesting to obtain an estimate of the value of δ_{CP} that is needed for reproducing the asymmetry (1.1) via (1.2), in either interpretation.

With one exception [35], simulations in 3+1 dimensions have not included CP violation. In [35] there was a search for an asymmetry induced by a chemical potential for Chern-Simons number. Technical difficulties were reported and no asymmetry was seen. Simulations in 1+1 dimensions similar to what we consider here were performed in [36, 16] and in more detail for the case of a tachyonic quench in [22]. In [22] we showed that the final asymmetry is proportional to the applied C violation (in 1+1 dimensions, C violation plays the role of CP violation in 3+1 dimensions), with an interesting dependence on the ratio of Higgs to W masses.

The structure of the rest of this paper is as follows: In section 2 we review scenarios for tachyonic preheating after inflation. In section 3 we describe the SU(2)-Higgs model with the added CP-violating term, and discuss the equations of motion. Section 4 is devoted to

the classical approximation and the details of the applied initial conditions. In section 5 we present our results. Finally, section 6 concludes with our estimate for the generated baryon asymmetry and the magnitude of δ_{CP} . Technical details can be found in the Appendix.

Preliminary accounts of this work have been given in [37, 38, 39, 31].

2. Tachyonic electroweak preheating

As mentioned in the Introduction, with regard to the magnitude of CP violation it is interesting to explore scenarios in which the electroweak transition took place at zero temperature. Let us assume that the effective mass parameter μ_{eff}^2 in the Higgs potential

$$V_\phi = V_0 + \mu_{\text{eff}}^2 \phi^\dagger \phi + \lambda(\phi^\dagger \phi)^2 \quad (2.1)$$

was at first positive and then turned negative (‘tachyonic’), ending up at the current value $-\mu^2$. We recall that μ is simply related to the Higgs mass, $\mu^2 = m_H^2/2$, and assume for the purpose of discussion that $\mu \approx 100$ GeV. We now discuss two realizations for the sign change of μ_{eff}^2 , firstly one that is instructive but that we will argue to be not viable, and secondly the more conventional one proposed in [18].

An elegant realization for μ_{eff}^2 could be a non-minimal coupling to the gravitational field,

$$\mu_{\text{eff}}^2 = \xi R - \mu^2, \quad (2.2)$$

with R the scalar curvature. As far as we know, there are no limits known yet on the parameter ξ . An indicative value is $\xi = 1/6$, the conformal case, so it is natural to assume $\xi \approx 1/6$. As an example, consider inflation in which R is initially large and positive, such that μ_{eff}^2 is positive. After inflation R goes down and μ_{eff}^2 goes through zero when $R \approx (100 \text{ GeV})^2$. The transition will take place somewhat later when the Hubble rate, which is generically of order $R^{1/2}$, has dropped sufficiently for the Hubble damping term in the Higgs-field e.o.m. ($3H\dot{\phi}$) to become subdominant, say $H \approx 1 - 10$ GeV. For $H \approx 1$ GeV, the energy density is still very large, $\rho = 3H^2 m_{\text{P}}^2 \approx (10^9 \text{ GeV})^4$ (we use $m_{\text{P}} = (8\pi G)^{-1/2}$), far above the electroweak scale of about $(100 \text{ GeV})^4$. After the transition the inflaton still dominates the energy and it should have released this into the SM degrees of freedom before big bang nucleosynthesis (BBN) can take over.

In the conventional scenario (see e.g. [40], section 8.3), the universe expands in matter-dominated fashion when the inflaton (σ) has fallen out of slow roll and is oscillating in the minimum of its potential, while decaying into the SM degrees of freedom (‘radiation’). The inflaton decay rate Γ_σ should be sufficiently slow, otherwise the maximum temperature in radiation [40],

$$T_{\text{max}} \simeq g_*^{-1/4} M_{\text{infl}}^{1/2} (\Gamma_\sigma m_{\text{P}})^{1/4}, \quad (2.3)$$

might rise above the electroweak transition temperature $T_c \approx 100$ GeV, and the sphaleron rate would wash out the generated asymmetry. Here g_* is the usual effective number of d.o.f and M_{infl} is the energy scale of inflation, which by the previous argument is larger than $\approx 10^9$ GeV. Requiring $T_{\text{max}} < 100$ GeV leads to $\Gamma_\sigma < 10^{-27}$ GeV. Such an extremely small decay rate is perhaps not unnatural if the inflaton resides in gravitational degrees

of freedom, and $(\xi - 1/6)^2$ is sufficiently small. However, it also leads to a reheating temperature [40]

$$T_{\text{rh}} \approx g_*^{-1/4} (\Gamma_\sigma m_{\text{P}})^{1/2} \quad (2.4)$$

that is smaller than 10^{-2} MeV, in conflict with BBN. Moreover, the entropy in a comoving volume produced by the decaying inflaton, $S = sa^3$ (s is the entropy density and a the scale factor), increases $\propto a^{15/8}$ [40], whereas the corresponding baryon number $B = n_B a^3$ is essentially conserved for $T < 100$ GeV. Then the crucial ratio n_B/s suffers dilution by a huge factor $(a_1/a_2)^{15/8} = (t_1/t_2)^{5/4} \approx 10^{-34}$, where $t_1 \approx m_{\text{P}}/M_{\text{infl}}^2$ is the time at the end of inflation and $t_2 \approx 1/\Gamma_\sigma$ the time the inflaton has decayed.

The numbers look better, but not good enough, if the inflaton potential does not have quadratic minimum but simply falls away such that the kinetic energy dominates (‘kinetion’), as in quintessential inflation [41]. In this case the energy density falls faster than the radiation in SM particles, $\rho_\sigma \propto a^{-6}$. However, going through a similar analysis leads to practically the same T_{rh} , an entropy growth $S \propto a^{3/4}$ and a dilution factor $\approx 10^{-8}$. In case Γ_σ is negligible, the entropy would be conserved and n_B/s would be constant. However, it then takes too long for the energy density in SM d.o.f., $\rho_{\text{SM}} \propto a^{-4}$, to become comparable to ρ_σ . This would happen at a temperature much too low for BBN: $T/T_1 = a_1/a = (\rho_{\text{SM}}/\rho_\sigma)_1^{1/2} \approx 10^{-14}$, or $T \approx 10^{-9}$ MeV.

These problems are avoided if the energy scales of inflation and radiation are comparable, specifically low-scale inflation with $M_{\text{infl}} \approx 100$ GeV. For this the realization (2.2) does not work (unless $\xi > 10^{26}$!). In [16, 17] a hybrid inflation mechanism was proposed in which the Higgs field is coupled to the inflaton,

$$\mu_{\text{eff}}^2 = \lambda_{\sigma\phi} \sigma^2 - \mu^2, \quad (2.5)$$

and σ was assumed to roll from large values towards $\sigma = 0$. Considering the effect of radiative corrections of the Higgs to the inflaton led [18] to the conclusion that inverted hybrid inflation is a better option (see also [42]),

$$\mu_{\text{eff}}^2 = \mu_\phi^2 - \lambda_{\sigma\phi} \sigma^2, \quad (2.6)$$

where now σ runs from 0 to $[(\mu^2 + \mu_\phi^2)/\lambda_{\sigma\phi}]^{1/2}$. An explicit example of the inflaton-Higgs potential is given in [18]:

$$V(\sigma, \phi) = V_0 - \frac{1}{5} \lambda_5 \sigma^5 + \frac{1}{6} \kappa_6 \sigma^6 + \frac{1}{2} (\mu_\phi^2 - \lambda_{\sigma\phi} \sigma^2) \phi^2 + \frac{1}{4} \lambda \phi^4 \quad (2.7)$$

(for simplicity for one real ϕ), with $\lambda_5 = 7.3 \times 10^{-5} \text{ GeV}^{-1}$, $\kappa_6 = 2.4 \times 10^{-7} \text{ GeV}^{-2}$, $\mu_\phi^2 = 1000 \text{ GeV}^2$, $\lambda_{\sigma\phi} = 0.04$, and V_0 such that $V = 0$ in its minimum, $V_0 \simeq (86 \text{ GeV})^4$.

Choosing $\lambda = 1/9$ leads to the vacuum expectation values $\langle \phi \rangle = 237 \text{ GeV}$ (reasonably close to the correct 246 GeV), $\langle \sigma \rangle = 426 \text{ GeV}$, and $\mu = 79 \text{ GeV}$. The inflaton-Higgs coupling $\lambda_{\sigma\phi}$ is quite strong, which causes substantial mixing in the minimum of the potential. The eigenvalues of the mass matrix are given by $(74 \text{ GeV})^2$ and $(147 \text{ GeV})^2$, differing considerably from the diagonal elements $\partial^2 V / \partial \sigma^2 = (121 \text{ GeV})^2$ and $\partial^2 V / \partial \phi^2 = (111 \text{ GeV})^2$, so one may wonder if the SM Higgs physics is not too much affected.

Another question that needs further investigation is the fact that in this model the inflaton decay width is much larger than the Hubble rate. At this low-scale inflation the Hubble rate is only $H \approx 10^{-5}$ eV, whereas one expects $\Gamma_\sigma \approx 1$ GeV. In the regime $\Gamma_\sigma \gg H$, *warm inflation* has been advocated [43], which puts into question our assumption of a cold universe after inflation.

However, the problems with the previous realization (2.2) are avoided. After the transition the inflaton decays rapidly into the SM d.o.f. via the mixing with the Higgs. Neglecting the tiny Hubble rate and using energy conservation, the ‘reheat’ temperature is approximately given by

$$T = \left(\frac{30}{\pi^2 g_*} \right)^{1/4} V_0^{1/4}. \quad (2.8)$$

With $g_* = 86.25$ for the effective number of d.o.f. below the W mass (leptons, quarks, gluons, photons), and a Higgs mass of, say, 160 GeV, this gives $T \simeq 51$ GeV, well above the BBN and QCD transition temperatures.

Because of the uncertainties in the specific realization of the assumed tachyonic electroweak transition, we model the transition by an instantaneous quench:

$$\begin{aligned} \mu_{\text{eff}}^2 &= +\mu^2, & t < 0, \\ &= -\mu^2, & t > 0. \end{aligned} \quad (2.9)$$

This is a limiting case of the transition in a finite time treated in [44, 23]. In this way we ‘shield’ the SM from the uncertainties of the inflaton and presumably, the quench will generate a maximal baryon asymmetry for a given amount of CP violation. Requiring zero vacuum energy gives

$$V_0 = \mu^4/4\lambda, \quad (2.10)$$

with a ‘reheat’ temperature similar to the model (2.7).

The initial state for the Higgs field is $\langle \phi \rangle = 0$ with $\mu_{\text{eff}}^2 > 0$. When $\mu_{\text{eff}}^2 < 0$ the Higgs field suffers the spinodal instability: $\langle \phi \rangle$ does not change, but its low momentum modes grow exponentially [22]. Soon the quartic term in the Higgs potential kicks in and eventually with the other SM couplings the fields will thermalize in the broken phase minimum. Initially there is rapid effective-thermalization [34], called ‘tachyonic preheating’ [45].

3. The SU(2)-Higgs model

To study the baryon asymmetry emerging after the electroweak transition we used the SU(2) Higgs model with effective CP violation, given by the action

$$\begin{aligned} S = - \int d^4x \left[\frac{1}{2g^2} \text{Tr} F_{\mu\nu} F^{\mu\nu} + (D_\mu \phi)^\dagger D^\mu \phi - \mu^2 \phi^\dagger \phi + \lambda (\phi^\dagger \phi)^2 + V_0 \right. \\ \left. + \kappa \phi^\dagger \phi \text{Tr} F^{\mu\nu} \tilde{F}_{\mu\nu} \right] \end{aligned} \quad (3.1)$$

Here $F_{\mu\nu} = \partial_\mu A_\nu - \partial_\nu A_\mu - i[A_\mu, A_\nu]$, $D_\mu \phi = (\partial_\mu - iA_\mu)\phi$, with ϕ the Higgs doublet, $\tilde{F}_{\mu\nu} = \epsilon_{\mu\nu\rho\sigma} F^{\rho\sigma}/2$, our metric is $(-1, 1, 1, 1)$ and $\epsilon_{0123} = +1$. As usual $A_\mu = A_\mu^a \tau^a/2$

with τ^a , $a = 1, 2, 3$, the Pauli matrices. The vacuum expectation value of the Higgs field is $|\langle\phi\rangle| = v/\sqrt{2}$, with $v = \mu/\sqrt{\lambda}$, and the Higgs and W masses are given by $m_H = \sqrt{2}\mu = \sqrt{2\lambda}v$, $m_W = gv/2$; $V_0 = \mu^4/4\lambda$. The magnitude of the effective CP violation is parametrized by κ . For later reference, we define the dimensionless

$$k = 16\pi^2\kappa m_W^2. \quad (3.2)$$

The equation of motion for the Higgs doublet is

$$\left(D_\mu D^\mu + \mu^2 - 2\lambda\phi^\dagger\phi - \kappa\text{Tr} F^{\mu\nu}\tilde{F}_{\mu\nu}\right)\phi = 0. \quad (3.3)$$

For the gauge fields the equations of motion are given by

$$D_0\left(\frac{1}{g^2}E_k^a - 2\kappa\phi^\dagger\phi B_k^a\right) - \epsilon_{klm}D_l\left(\frac{1}{g^2}B_m^a + 2\kappa\phi^\dagger\phi E_m^a\right) + j_k^a = 0, \quad (3.4)$$

where $E_k^a = F_{k0}^a$ and $B_k^a = \epsilon_{klm}F_{lm}^a/2$ are the SU(2) electric and magnetic fields, D_k is the covariant derivative in the adjoint representation, e.g.

$$D_\mu B_k^a = \partial_\mu B_k^a + \epsilon_{abc}A_\mu^b B_k^c, \quad (3.5)$$

and j_μ^a is the Higgs contribution to the SU(2) current

$$j_\mu^a = i(D_\mu\phi)^\dagger\frac{\tau^a}{2}\phi - i\phi^\dagger\frac{\tau^a}{2}D_\mu\phi. \quad (3.6)$$

In addition, the Gauss constraints have to be satisfied,

$$D_k\left(\frac{1}{g^2}E_k^a - 2\kappa\phi^\dagger\phi B_k^a\right) + j_0^a = 0. \quad (3.7)$$

If these conditions hold at one time, they hold at all times as a consequence of the equations of motion (3.4).

If $\phi^\dagger\phi$ were constant, the CP-violating terms are ineffective, since then the κ -term in the action is the integral of a total derivative,

$$\text{Tr} F_{\mu\nu}\tilde{F}^{\mu\nu} = 16\pi^2\partial_\mu j_{\text{CS}}^\mu, \quad (3.8)$$

where j_{CS}^μ is the Chern-Simons current

$$j_{\text{CS}}^\mu = \frac{1}{32\pi^2}\epsilon^{\kappa\lambda\mu\nu}\left(A_\lambda^a F_{\mu\nu}^a - \frac{1}{3}\epsilon_{abc}A_\lambda^a A_\mu^b A_\nu^c\right). \quad (3.9)$$

Similarly, for constant $\phi^\dagger\phi$, the κ terms drop out of the field equations because of the Bianchi identities $\epsilon^{\kappa\lambda\mu\nu}D_\lambda F_{\mu\nu}^a = 0$. Hence, an alternative version of (3.4) and (3.7) is

$$0 = D_0 E_k^a - 2g^2\kappa B_k^a\partial_0(\phi^\dagger\phi) - \epsilon_{klm}D_l B_m^a - 2g^2\kappa\epsilon_{klm}E_m^a\partial_l(\phi^\dagger\phi) + g^2 j_k^a, \quad (3.10)$$

$$0 = D_k E_k^a - 2g^2\kappa B_k^a\partial_0(\phi^\dagger\phi) + g^2 j_0^a, \quad (3.11)$$

respectively.

4. Initial conditions and classical approximation

We consider an initial state where the Universe is at zero temperature, with the Higgs field expectation value at zero. In the vacuum, there are quantum fluctuations, and we would like to use those to seed the Higgs symmetry breaking. Several ways have been suggested (see for instance [19, 46]). We follow the line described in [22] (see also [21] for the more realistic case of a rapid but not instantaneous quench), by solving the quantum evolution in the limit of zero coupling, $\lambda = 0$. We also neglect the interactions with the gauge fields for the moment. In this limit, the Higgs potential after the quench at $t = 0$ is just an inverted parabola

$$V(\phi) = V_0 - \mu^2 \phi^\dagger \phi = V_0 - \frac{1}{2} \mu^2 \phi_\alpha \phi_\alpha \quad (4.1)$$

where the ϕ_α , $\alpha = 1, 2, 3, 4$, are four real fields representing the complex Higgs doublet. For the moment we consider just one of those real components. It is straightforward to solve the operator equations of motion for $t > 0$ with the initial condition that the field is free with mass μ for times $t < 0$. In terms of Fourier modes

$$\phi_{\mathbf{k}} = \int d^3x \frac{e^{-i\mathbf{k}\cdot\mathbf{x}}}{\sqrt{L^3}} \phi(\mathbf{x}) \quad (4.2)$$

in a periodic volume L^3 , one then finds that modes with $k < \mu$ are unstable and grow exponentially. For $\sqrt{\mu^2 - k^2} t \gg 1$,

$$\phi_{\mathbf{k}} \propto \exp\left(\sqrt{\mu^2 - k^2} t\right), \quad (4.3)$$

and the particle numbers of the unstable modes in the initial state $|0\rangle$ (the vacuum for $t < 0$) also grow exponentially. So these dominating modes become classical and indeed, the expectation value of generic products of field operators can be reproduced by a classical gaussian distribution [22],

$$P(\xi) \propto \exp\left[-\frac{1}{2} \sum_{|\mathbf{k}| < \mu} \left(\frac{|\xi_{\mathbf{k}}^+|^2}{n_k + 1/2 + \tilde{n}_k} + \frac{|\xi_{\mathbf{k}}^-|^2}{n_k + 1/2 - \tilde{n}_k}\right)\right], \quad (4.4)$$

$$\xi_{\mathbf{k}}^\pm = \frac{1}{\sqrt{2\omega_k}} (\omega_k \phi_{\mathbf{k}} \pm \pi_{\mathbf{k}}), \quad (4.5)$$

where π is the canonical conjugate to ϕ . The particle numbers n_k , \tilde{n}_k and frequencies ω_k are defined in terms of the two-point functions

$$\langle \pi_{\mathbf{k}} \pi_{\mathbf{k}}^\dagger \rangle = \left(n_k + \frac{1}{2}\right) \omega_k, \quad (4.6)$$

$$\langle \phi_{\mathbf{k}} \phi_{\mathbf{k}}^\dagger \rangle = \left(n_k + \frac{1}{2}\right) \frac{1}{\omega_k}, \quad (4.7)$$

$$\langle \pi_{\mathbf{k}} \phi_{\mathbf{k}}^\dagger \rangle = \langle \pi_{\mathbf{k}} \phi_{\mathbf{k}}^\dagger \rangle + i = \tilde{n}_k + \frac{i}{2}, \quad (4.8)$$

which can be calculated to be [22]

$$\langle \phi_{\mathbf{k}} \phi_{\mathbf{k}}^\dagger \rangle = \frac{1}{2\omega_k^+} \left[1 + \left(\frac{\omega_k^{+2}}{\omega_k^{-2}} - 1 \right) \sin^2(\omega_k^- t) \right], \quad (4.9)$$

$$\langle \pi_{\mathbf{k}} \pi_{\mathbf{k}}^\dagger \rangle = \frac{\omega_k^{-2}}{2\omega_k^+} \left[1 + \left(\frac{\omega_k^{+2}}{\omega_k^{-2}} - 1 \right) \cos^2(\omega_k^- t) \right], \quad (4.10)$$

$$\langle \pi_{\mathbf{k}} \phi_{\mathbf{k}}^\dagger \rangle = \frac{\omega_k^-}{4\omega_k^+} \left(\frac{\omega_k^{+2}}{\omega_k^{-2}} - 1 \right) \sin(2\omega_k^- t) + \frac{i}{2}, \quad (4.11)$$

$$\omega_k^\pm = \sqrt{\pm\mu^2 + k^2}. \quad (4.12)$$

Explicit expressions for n_k , \tilde{n}_k and ω_k are easily obtained, which show that for $|\omega_k^-|t > 1$, $n_k + 1/2 + \tilde{n}_k$ grows exponentially, whereas the difference $n_k + 1/2 - \tilde{n}_k$ rapidly approaches zero (see figure 2 in [22]). This means that the typical $\xi_{\mathbf{k}}^+$ grows exponentially and the typical $\xi_{\mathbf{k}}^- \rightarrow 0$. In terms of $\phi_{\mathbf{k}}$ and $\pi_{\mathbf{k}}$ the distribution gets squeezed.

It therefore makes sense to treat the dynamics classically, as soon as the particle numbers are large, $n_k \gg 1/2$. This is the case for sufficiently long “roll-off” times, keeping in mind that the quadratic approximation will break down when the interaction terms becomes non-negligible. For a given choice of “roll-off” time and thus n_k , \tilde{n}_k and ω_k , we reproduce generic quantum correlators of the initial conditions by an ensemble of random classical initial field configurations. These can then be evolved using the classical equations of motion. In this classical approximation the quantum averages are replaced by averages over the initial ensemble.

The classical evolution can be carried out on a computer, including fully the non-linear interactions. This assumes of course that the particle numbers in the gauge fields will also grow large, such that they can also be treated classically. A large growth of gauge field modes could be seen *a posteriori*. In [34], we found that the Higgs occupation numbers for the unstable modes indeed become very large ($n_0 \approx 100$) during the instability. In addition, the gauge fields also acquire large occupation numbers, thereby supporting the classical approximation for the whole system, at least for the time scales under consideration here. The large particle numbers in the gauge field modes suggest that our major observable to be computed, $\langle N_{\text{CS}}(t) - N_{\text{CS}}(0) \rangle$, can also be obtained reasonably accurately in the classical approximation.

The Gauss constraints (3.7) need to be imposed on the initial conditions. We do this as follows. As long as the free-field approximation is valid, the gauge fields cannot feel the exponential growth of the Higgs fields, so we initialize $A_\mu^a = 0$. Then the covariant derivative in (3.7) reduces to an ordinary derivative and it is straightforward to solve for the electric field components, E_k^a , given the Higgs charge densities j^{0a} drawn from the distribution (4.4). However, before doing so one constraint has to be imposed first: in finite volume the global charge vanishes,

$$\int d^3x j_0^a = \int d^3x \partial_k F_{0k}^a / g^2 = 0. \quad (4.13)$$

We thus modify the distribution (4.4),

$$P(\xi) \rightarrow P(\xi) \delta(\mathbf{G}), \quad (4.14)$$

where $\delta(\mathbf{G})$ encodes this global Gauss constraint. This makes the distribution not quite Gaussian. For details see appendix B.

We will apply two types of initial conditions, dubbed ‘Just-a-half’ and ‘Thermal’. For additional details on these schemes, see [22].

4.1 Just-the-half distribution

In the quadratic approximation, classical and quantum evolution is identical, and we can therefore choose to sample the initial distribution (4.4, 4.14) at “roll-off” time zero, when the n ’s and ω ’s are simply given by

$$n_k = \tilde{n}_k = 0, \quad \omega_k = \sqrt{\mu^2 + k^2}. \quad (4.15)$$

leaving just the $1/2$ in the denominators in (4.4). We only initialize momentum modes that are unstable and that will acquire large occupation numbers under the spinodal instability, so $|\mathbf{k}| < \mu$. This also avoids initializing modes close to the lattice cut-off scale [46]. We name these initial conditions: Just-the-half.

4.2 Thermal distribution

A different condition is obtained from an initial state that is thermal but at a low temperature $T \ll m_H$. We consider this possibility to get some indication of the sensitivity of the results to the initial conditions. The initial particle numbers of the Higgs fields are chosen to be Bose-Einstein distributed:

$$n_k = (\exp(\omega_k/T) - 1)^{-1}, \quad \tilde{n}_k = 0, \quad \omega_k = \sqrt{\mu^2 + k^2}, \quad (4.16)$$

We use $T/m_H = 1/10$. In this case we initialize all the modes, not only the unstable ones, but of course, only the unstable ones will grow. In practice the large-momentum tail is so suppressed that it should make little difference to introduce the cut-off $k < \mu$. We name these initial conditions: Thermal.

5. Numerical simulation

For the numerical simulation we translated the action to a lattice in (Lorentzian) space-time according to the usual method of lattice gauge theory, from which the discretized field equations follow in the standard fashion. The Gauss constraint (3.7) is compatible with the discretization and since the initial $A_0 = 0$, it stays zero and we are using temporal gauge. Because of the CP-violating terms the numerical algorithm for the equations of motion turns out to be ‘implicit’, causing it to be rather computer-expensive. Lattice details are given in the appendix.

We evolved ensembles of 45 initial conditions in time using classical dynamics. In two cases (Thermal initial conditions, $k \equiv 16\pi^2\kappa m_W^2 = 0$ and 3) we averaged over larger

ensembles of about 300 configurations. We used volumes $(Lm_H)^3 = 21^3$ with periodic boundary conditions, and a spatial lattice spacing $am_H = 0.35$, so with 60^3 lattices. This is a compromise between computer time and capacity and the need to have enough unstable modes on the lattice. Here, we have about 50 such modes. Also, we found that with this choice of lattice spacing discretization errors in the Chern-Simons number and Higgs-winding number (see below) were small enough for our purpose.

5.1 Observables

The spatial average of $\phi^\dagger\phi$,

$$\overline{\phi^\dagger\phi} \equiv \frac{1}{L^3} \int d^3x \phi^\dagger\phi, \quad (5.1)$$

is a good indicator for the development of the instability in time. Our most important observable is the Chern-Simons number

$$N_{\text{CS}} = \int d^3x j_{\text{CS}}^0, \quad (5.2)$$

since the change in time of its expectation value determines the baryon asymmetry through eq. (1.2),

$$B(t) = 3\langle N_{\text{CS}}(t) - N_{\text{CS}}(0) \rangle = 3 \int_0^t dx^0 \int d^3x \langle \partial_\mu j_{\text{CS}}^\mu \rangle = \frac{3}{8\pi^2} \int_0^t dx^0 \int d^3x \langle E_k^a B_k^a \rangle. \quad (5.3)$$

Another interesting observable is the winding number in the Higgs field

$$N_{\text{w}} = \frac{1}{24\pi^2} \int d^3x \epsilon_{klm} \text{Tr} \left(\partial_k V V^\dagger \partial_l V V^\dagger \partial_m V V^\dagger \right), \quad (5.4)$$

$$V = \frac{(i\tau^2 \phi^*, \phi)}{\phi^\dagger\phi} \in \text{SU}(2). \quad (5.5)$$

For configurations near equilibrium with low energy in the covariant Higgs derivatives, the gauge field is not far from being pure-gauge, $A_\mu \simeq -i\partial_\mu V V^\dagger$, and then $N_{\text{CS}} \simeq N_{\text{w}}$.

Observables such as the Chern-Simons number and the winding number are notoriously difficult to implement on the lattice in the quantum theory, but they turn out to be manageable in our classical approximation because the high-momentum modes are suppressed in the initial conditions.

5.2 Single trajectories

We evolved the initial configurations to time $t = 100 m_H^{-1}$, and computed the volume-averaged Higgs field $\overline{\phi^\dagger\phi}$, the Chern-Simons number N_{CS} and the Higgs winding number N_{w} . The initial Chern-Simons number was set to zero, so we really computed its change through eq. (5.3), which is gauge invariant.

Fig. 1 shows the observables versus time from a single such trajectory in configuration space. We see that $\overline{\phi^\dagger\phi}$ “falls off the hill into its broken phase minimum”, where it performs a damped oscillation as the energy becomes slowly distributed over the higher momentum modes. Meanwhile, the Chern-Simons number and winding number bounce around, until

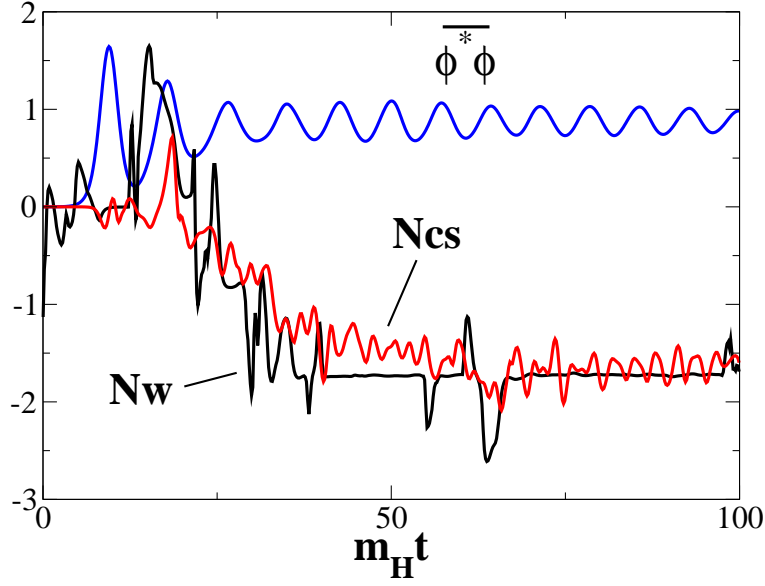


Figure 1: Volume-averaged Higgs field $2\overline{\phi^\dagger\phi}/v^2$, Chern-Simons number and winding number, for a typical trajectory with Thermal initial conditions, $m_H/m_W = 1$, and no CP violation, $k = 0$.

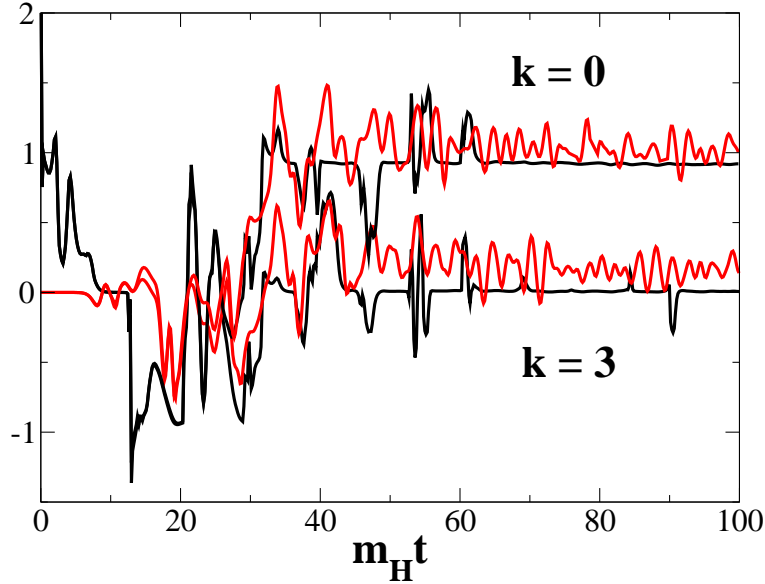


Figure 2: Example of N_{CS} and N_w for two trajectories with the same initial conditions, without ($k = 0$) and with ($k = 3$) CP violation. Thermal initial conditions, $m_H/m_W = 1$.

they settle near the same integer value (for N_w the difference with the integer is a finite-lattice spacing effect). The winding number appears to settle first and then the Chern-Simons number approaches it somewhat later.

In Fig. 2 we show a particular initial configuration evolved with and without CP violation. In this case, the final Chern-Simons number and winding number are shifted approximately by an integer (1) under the influence of CP violation. It is these shifts that

will give us a net Chern-Simons number asymmetry. Due to the chaotic nature of the equations of motion the shifts cannot be predicted from the magnitude of the CP violation (for example, in figure 2 the final $N_{CS} \simeq 1$ for $k = 0$ and $\simeq 0$ for $k = 3$). However, on the average, more shifts happen to one side than to the other.

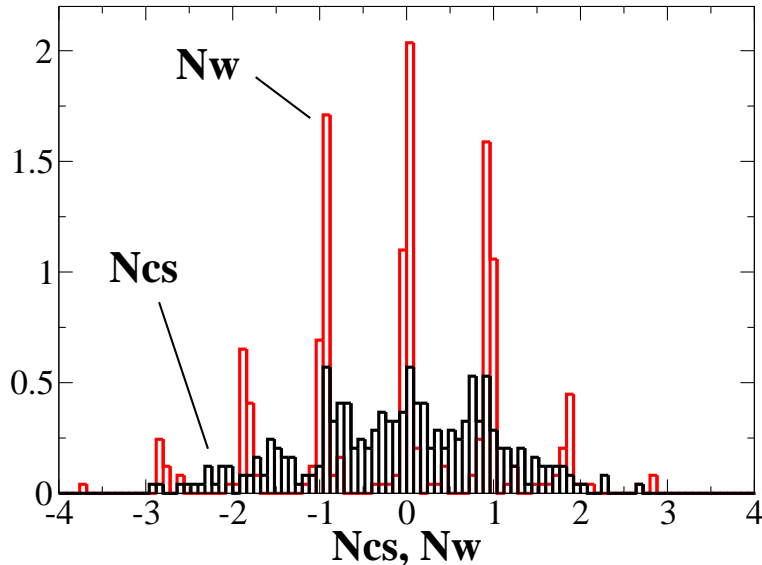


Figure 3: The distribution of final N_{CS} and N_w ; Thermal initial conditions, $m_H/m_W = 1$, no CP violation ($k = 0$), 303 configurations.

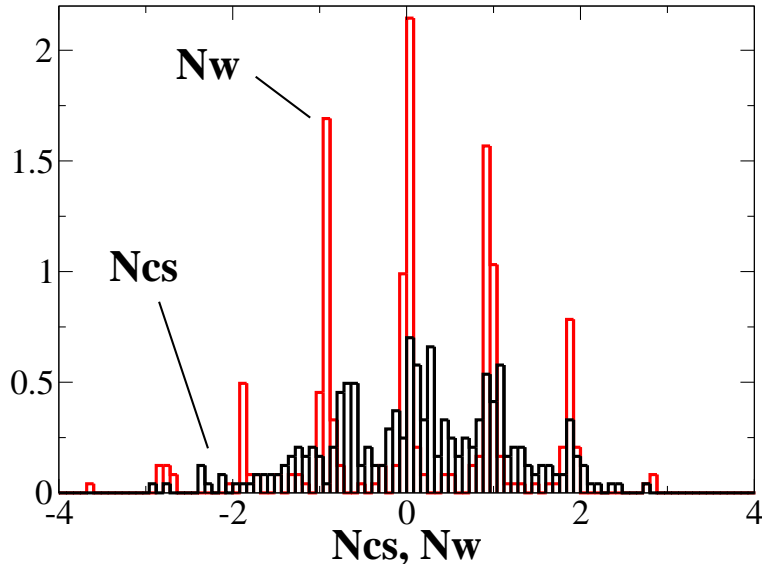


Figure 4: As in figure 3 with CP violation, $k = 3$.

Fig. 3 shows the distribution of final Chern-Simons number and winding number. Although both observables cluster around integers, the winding number is more peaked. The relatively short evolution time ($m_H t_{\text{final}} = 100$) does not allow Chern-Simons numbers

to settle completely. Furthermore, the system has a non-zero effective temperature, so the Chern-Simons numbers need not be integer. We have checked for a few configurations, that the Chern-Simons number settles eventually, sometimes as late as $m_H t = 500$. For most cases the Chern-Simons number is stuck already at time $m_H t = 100$.

Fig. 4 shows the final distributions when adding CP violation. Note that the initial configurations in Figs. 3 and 4 are exactly the same. It is not obvious that anything has changed and to spot the asymmetry we have to form ensemble-averaged quantities.

5.3 Ensemble averages

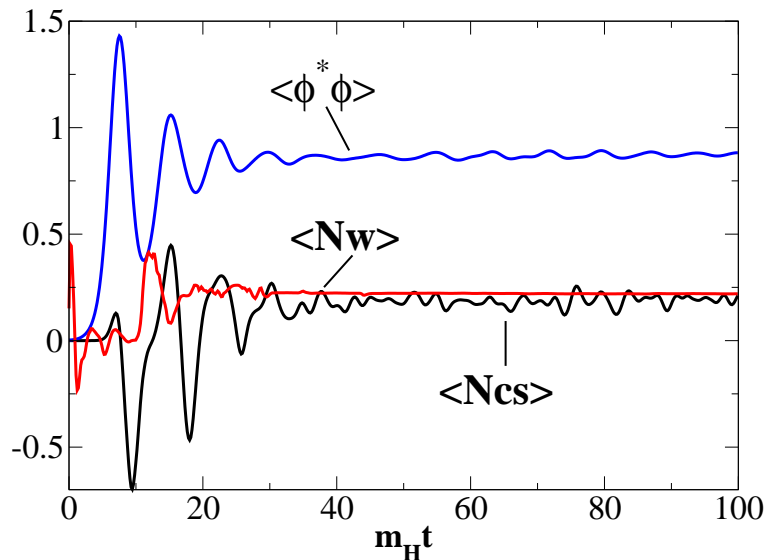


Figure 5: Averaged observables: $2\langle\overline{\phi^\dagger\phi}\rangle/v^2$, $\langle N_{CS} \rangle$ and $\langle N_w \rangle$ versus time for $m_H/m_W = 1$, Just-a-half initial conditions and $k = 8$.

In Fig. 5 we plot the ensemble averaged Higgs expectation value, Chern-Simons number and winding number vs. time. We see that the average Higgs field damps more strongly. The Chern-Simons number oscillates with a large amplitude before settling down. The oscillations seem to be driven by the oscillations in the Higgs field. At the end, both observables settle at non-zero values. Fig. 6 shows the average Chern-Simons numbers for different values of k . Notice that the oscillations have larger amplitude with larger k .

Fig. 7 sums up our results and the dependencies on the parameters. We keep m_W fixed and plot $\langle N_{CS} \rangle / (L m_W)^3$ vs. k at $m_H t = 100$. The dependence on initial conditions appears to be weak. There is a hint of a dependence on mass ratio m_H/m_W .

The dependence on k is not linear for the Thermal, $m_H/m_W = 1$, case. We have observed similar non-linear behavior for large κ (large C -violation) in the 1+1 D Abelian Higgs model, but were able to establish linearity at smaller κ . Here a linear regime presumably also exists at small k , but it is unclear where it ends. We lack sufficient statistics to draw a conclusion. Still, a linear fit through the origin is consistent with the data for $k \leq 10$ (dashed lines), for the $m_H = \sqrt{2} m_W$ case ($\chi^2/\text{d.o.f} = 0.25$) and less so for $m_H = m_W$

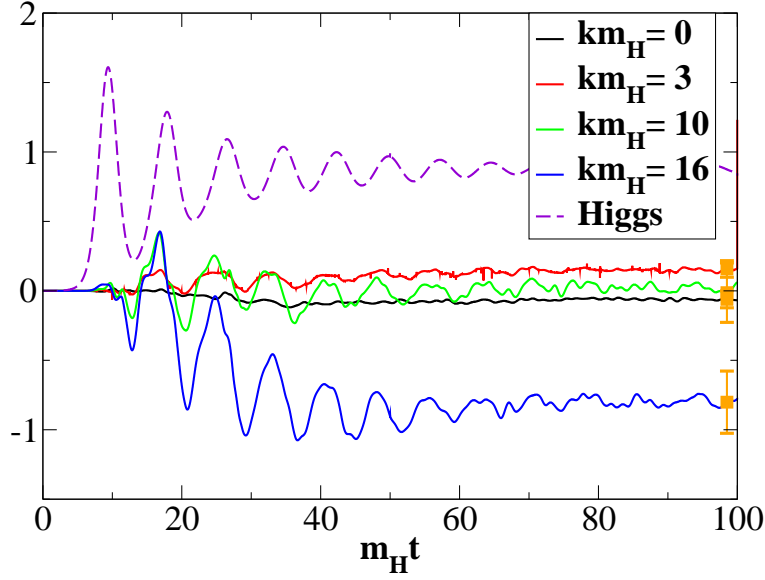


Figure 6: Expectation values $2\langle\overline{\phi^\dagger\phi}\rangle/v^2$ and $\langle N_{CS}\rangle$ for different k ; $m_H/m_W = 1$ and Thermal initial conditions.

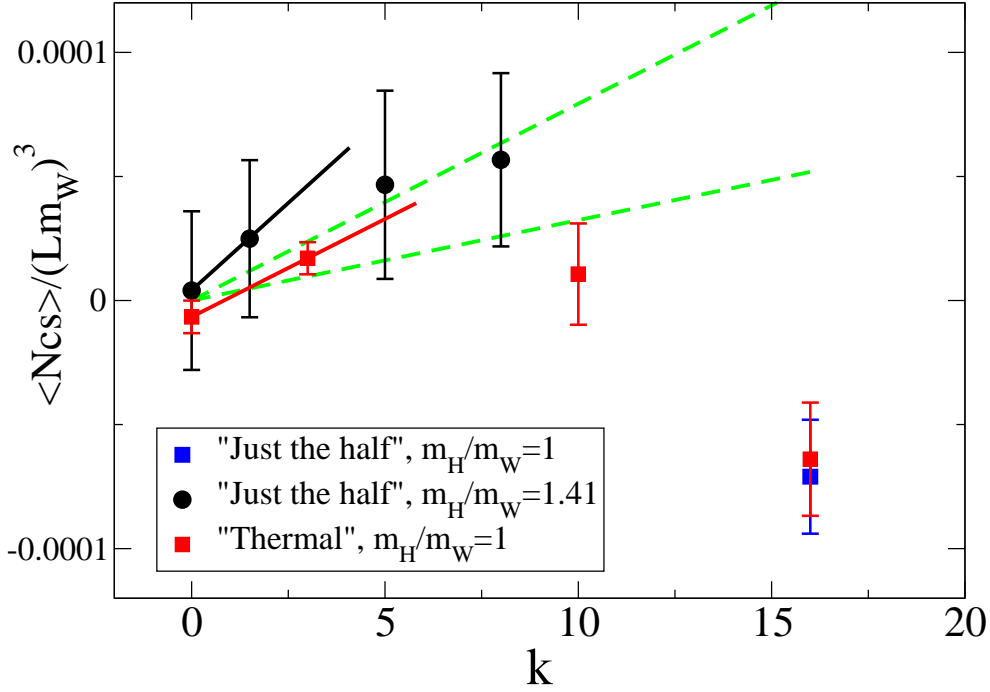


Figure 7: Results for the Chern-Simons density all k , m_H/m_W and initial conditions. The full lines represent linear fits through the two points with lowest k : $k = 0, 3$ ($m_H = m_W$) and $k = 0, 1.5$ ($m_H = \sqrt{2}m_W$). The dashed lines are linear fits through the origin, ignoring the data at $k = 0$, and also at $k = 16$ for the case $m_H = m_W$.

($\chi^2/\text{d.o.f} = 2.4$),

$$\frac{\langle N_{CS}\rangle}{(Lm_W)^3} = (0.32 \pm 0.15) \times 10^{-5} k, \quad m_H = m_W, \quad (5.6)$$

$$= (0.79 \pm 0.36) \times 10^{-5} k, \quad m_H = \sqrt{2} m_W. \quad (5.7)$$

This fit takes into account that with infinite statistics the result at $k = 0$ should be zero. However, the large χ^2 in the $m_H = m_W$ case suggests contamination from non-linear behavior.

To diminish the uncertainty of where the linear regime ends we focus on the lowest k -values, $k = 0, 3$, $m_H = m_W$, and $k = 0, 1.5, 3$, $m_H = \sqrt{2} m_W$. We expect these points to be close to, or in, the linear regime that is of physical relevance. Furthermore, since we used exactly the same initial configurations for the data at $k = 0$ and at $k = 1.5, 3$, the effect of CP violation is the *difference* between the zero and non-zero k results. An overall shift due to finite statistics cancels out in this difference. These fits are represented by the continuous lines in figure 7. The fitted slopes are given by

$$\frac{\langle N_{CS} \rangle}{(Lm_W)^3} = (0.79 \pm 0.31) \times 10^{-5} k, \quad m_H = m_W, \quad (5.8)$$

$$\simeq 1.4 \times 10^{-5} k, \quad m_H = \sqrt{2} m_W. \quad (5.9)$$

The error in the $m_H = m_W$ case is obtained by shifting the data upward with the negative of the $k = 0$ value and combining the errors at $k = 3$ in quadrature. For the case $m_H = \sqrt{2} m_H$ this would lead to a too large, not meaningful error, which we have left out. We consider as our best estimate for the slope the result (5.7) from the previous fit (upper dashed line in figure 7), keeping in mind that this is perhaps an under-estimate because of the apparent curvature in the data.

5.4 Initial rise

It is clearly difficult to predict the final averaged Chern-Simons number analytically. For early times, specifically during the very first roll-off of the Higgs field, we can however understand the asymmetry generated by the driving force of the CP-violating term, through an analysis similar to that used in the analog 1+1 D Abelian Higgs model [22]. Consider a spatial region in which the fields are gauge-equivalent to being homogeneous and choose a gauge in which they actually are homogeneous. For homogeneous fields, the equations of motion for the gauge field read:

$$\partial_t^2 A_k^a = A_k^b A_l^b A_l^a - A_k^a A_l^b A_l^b - \frac{1}{2} g^2 A_k^a \phi^\dagger \phi - 2g^2 \kappa B_k^a \partial_t(\phi^\dagger \phi) \quad (5.10)$$

In the Abelian Higgs model in 1+1 dimensions [22], the simplicity of the C-bias term ensures that the gauge field does not enter into the driving force (the κ -term). In the present case, however, its effect is suppressed by

$$B_k^a = \frac{1}{2} \epsilon_{klm} \epsilon_{abc} A_l^b A_m^c. \quad (5.11)$$

To estimate the asymmetry, we assume that the Higgs field, which may be viewed as an O(4) vector, rolls off the quadratic potential, say in the direction ϕ_3 :

$$\partial_t^2 \phi_3 = \mu^2 \phi_3 \rightarrow \phi^\dagger \phi = \phi_0^2 e^{2\mu t}. \quad (5.12)$$

Assume that we have solved the system for $\kappa = 0$. From the simulations, we know that the gauge field also grows exponentially, say

$$A_{k,0}^a = C_k^a e^{c\mu t}. \quad (5.13)$$

We perturb with the κ term, and write

$$A_k^a = A_{k,0}^a + \kappa A_{k,1}^a. \quad (5.14)$$

Then the equation for the perturbation $A_{k,1}^a$ is

$$\partial_t^2 A_{k,1}^a = -H_{kl}^{ab} A_{l,1}^b - 2g^2 B_{k,0}^a \partial_t(\phi^\dagger \phi), \quad (5.15)$$

with

$$H_{kl}^{ab} = (A^2 \delta_{kl} - A_k^c A_l^c) \delta_{ab} - A_m^a A_m^b \delta_{kl} + 2A_k^a A_l^b - A_l^a A_k^b + \frac{1}{2} g^2 \phi^\dagger \phi \delta_{kl} \delta_{ab}, \quad (5.16)$$

evaluated at zeroth order in κ . For small times H is dominated by the $\phi^\dagger \phi$ term, which acts like an effective-frequency term for the perturbation, that will turn the initial rise induced by the source term $\propto \partial_t(\phi^\dagger \phi)$ into the small initial bump in figures 5 and 6. Assuming this effective mass term can be neglected at early times we can integrate (5.15) using (5.12) and (5.13) and express the result as

$$A_{k,1}^a = -\frac{2\mu}{(2\mu + 2c\mu)^2} 2g^2 B_{k,0}^a \phi^\dagger \phi. \quad (5.17)$$

For homogeneous fields the Chern-Simons density is given by (cf. (3.9))

$$n_{\text{CS}}(t) = \int_0^t dx^0 \partial_0 j_{\text{CS}}^0 = -\frac{1}{48\pi^2} \epsilon_{klm} \epsilon_{abc} A_k^a A_l^b A_m^c \quad (5.18)$$

evaluated at time t . Averaging over initial conditions the zeroth order contribution in κ will vanish and we get

$$\langle n_{\text{CS}} \rangle = -\kappa \frac{1}{8\pi^2} \langle B_{k,0}^a A_{k,1}^a \rangle = \frac{\kappa g^2}{8\pi^2 (1+c)^2 \mu} \langle B^2 \phi^\dagger \phi \rangle. \quad (5.19)$$

We now assume this expression, which was derived for our homogenous patch, to be independent of where the patch was located, and replace $\langle B^2 \phi^\dagger \phi \rangle \rightarrow \langle \overline{B^2} \rangle \langle \overline{\phi^\dagger \phi} \rangle$, where $\langle \overline{B^2} \rangle$ and $\langle \overline{\phi^\dagger \phi} \rangle$ stand for the average over the volume as well as over initial conditions. This gives for the density in W-mass units,

$$\frac{\langle n_{\text{CS}} \rangle}{m_W^3} = \frac{\sqrt{2} k}{(8\pi^2)^2 (1+c)^2} \frac{\langle \overline{B^2} \rangle \langle \overline{\phi^\dagger \phi} \rangle (2/v^2)}{m_W^3 m_H}. \quad (5.20)$$

Using the computed values of $\langle \overline{B^2} \rangle$ and $\langle \overline{\phi^\dagger \phi} \rangle$, and inferring c from the measured behavior $\langle \overline{B^2} \rangle \propto \exp(4c\mu t)$, we can compare (5.20) to the data. For c we find $c \simeq 0.67$.

Fig. 8 shows the initial bump for $m_H/m_W = \sqrt{2}$, for varying k . The inset shows a comparison with the estimate (5.20), evaluated at a time for which $\langle \overline{\phi^\dagger \phi} \rangle = v^2/6$, the value

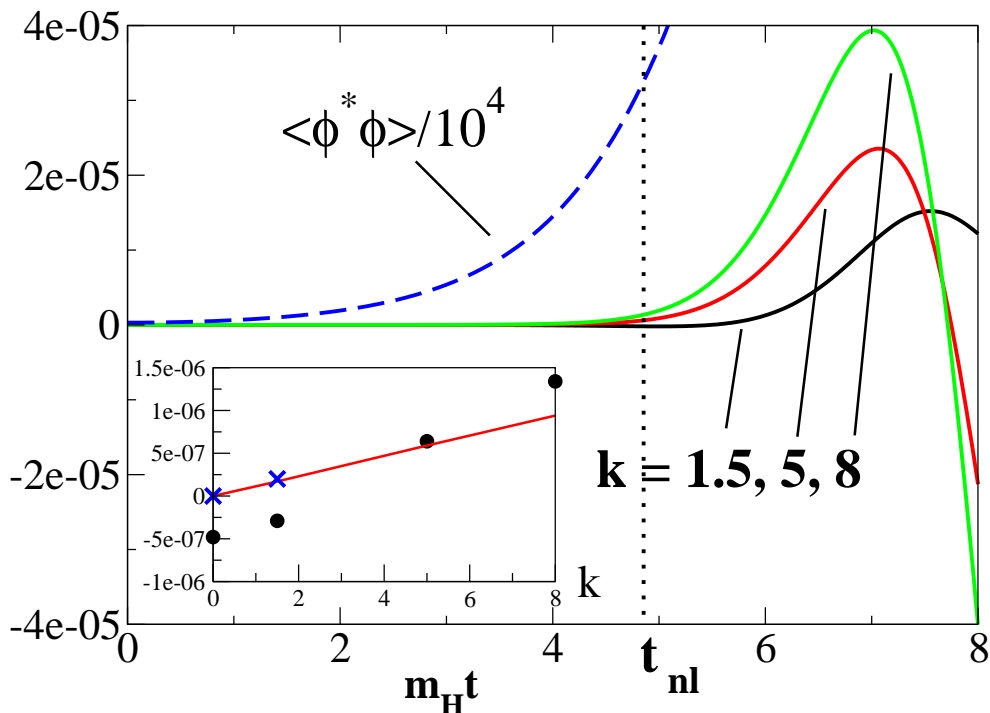


Figure 8: The initial rise for various k 's. The inset shows the size of the bump versus k for the estimate (5.20) (line), the results of the simulations (dots) and results shifted by the negative of the value at zero k (see main text); $m_H/m_W = \sqrt{2}$.

at which the curvature in the Higgs potential changes sign and the quadratic approximation (5.12) will be become more strongly affected by non-linearities. Because of finite statistics, there is an overall shift of the results that can be read off from the $k = 0$ simulation, which should give zero with an infinite number of initial configurations. In this case the $k = 0$ and 1.5 simulations started from the exact same initial conditions, and so we shift the $k = 0$ result to zero, and the $k = 3$ result by the same amount (as we did in section 5.3). These are the crosses in the inset. The agreement of (5.20) with the data is surprisingly good, given the approximations made.

5.5 Final temperature and sphaleron wash-out

In order for baryogenesis to be successful, we need the final temperature after symmetry breaking to be low enough so that an asymmetry does not get washed out by equilibrium sphaleron processes. The usual requirement for avoiding subsequent wash-out, namely, that the sphaleron energy is much larger than the temperature, can be conservatively formulated as [12] $v/T > 1.49$, or $T/v = 0.67$. The estimate (2.8), based on distributing the Higgs potential energy ($V_0 = v^2 m_H^2/8$) over g_* relativistic degrees of freedom, leads to

$$\frac{T}{v} = 0.442 \left(\frac{m_H}{v} \right)^{1/2}, \quad (5.21)$$

where we used $g_* = 10$ for the Higgs and W degrees of freedom. With $v = 246$ GeV and a Higgs mass in the range 114 – 200 GeV [7], the requirement is amply satisfied. For

example, for $m_H = \sqrt{2}m_W \simeq 114$ GeV the estimated temperature is $T = 74$ GeV.

In fact, our system is not yet in equilibrium after the transition and our particles are not massless. In [34] we computed Higgs and W particle numbers using the field configurations produced in our numerical simulation, from which we obtained effective temperatures and chemical potentials by comparing to a Bose–Einstein distribution. We found

$$\frac{T_{\text{eff}}}{m_H} \simeq 0.4, \quad \frac{\mu_{\text{eff}}^{\text{ch}}}{m_H} \simeq 1, \quad m_H = \sqrt{2}m_W. \quad (5.22)$$

At first glance this temperature should keep us safe from equilibrium sphaleron wash-out. The implied temperature $0.4 \times 114 = 45$ GeV is lower than the 74 GeV found above, which can be ascribed to the occurrence of the chemical potential. However, this large chemical potential implies that the occupation numbers are still very large for the low momentum modes, $n_k = [\exp(\sqrt{m^2 + k^2}/T - \mu^{\text{ch}}/T) - 1]^{-1} \gg 1$. Since these modes are the ones responsible for sphaleron processes, the actual rate may be larger than one would expect from the temperature alone.

In the Standard Model, the W and Higgs particles decay into the lighter particles, which will rapidly lead to a lowering of the temperature. For the W, the decay width is about 3 GeV and the Higgs width is expected to be similar, so that in a time span of a few hundred m_H^{-1} these particles have decayed. We do not see any wash-out on time scales of a few hundred m_H^{-1} . Then the final temperature will be determined by light degrees of freedom and thus close to the estimate (2.8) with the somewhat more favorable $g_* = 86.25$:

$$\frac{T}{v} = 0.258 \left(\frac{m_H}{v} \right)^{1/2} \quad (5.23)$$

(and a temperature $T = 43$ GeV for $m_H = 114$ GeV). We do not see a problem with wash-out.

5.6 Effective sphaleron rate

In [16] an effective sphaleron rate was introduced and used in estimating the effect of the CP-bias term using quasi-equilibrium concepts,

$$n_B \approx \frac{\delta_{\text{CP}}}{M^2} \Gamma_{\text{eff}} \frac{\langle \phi^\dagger \phi \rangle}{T_{\text{eff}}}, \quad (5.24)$$

where $\delta_{\text{CP}}/M^2 = 16\pi^2\kappa/3$ and T_{eff} is an effective temperature estimated to be about 350 GeV. This effective sphaleron rate was computed recently [23], with parameters different from ours (and with a finite quenching rate), and it is interesting to see its behavior in our simulation. The effective rate per unit volume can be defined as

$$\Gamma_{\text{eff}} = \frac{1}{L^3} \frac{d}{dt} [\langle N_{\text{CS}}(t)^2 \rangle - \langle N_{\text{CS}}(t) \rangle^2], \quad (5.25)$$

where we set $N_{\text{CS}} = 0$ at $t = 0$. In Fig. 9 we show Γ_{eff} versus time. It turns out to be insensitive to the choice of initial conditions, and insensitive to m_H/m_W . In equilibrium this quantity is the diffusion rate of Chern-Simons number, in which case it is the slope of a straight line approximating $\langle N_{\text{CS}}^2 \rangle - \langle N_{\text{CS}} \rangle^2$ (see inset).

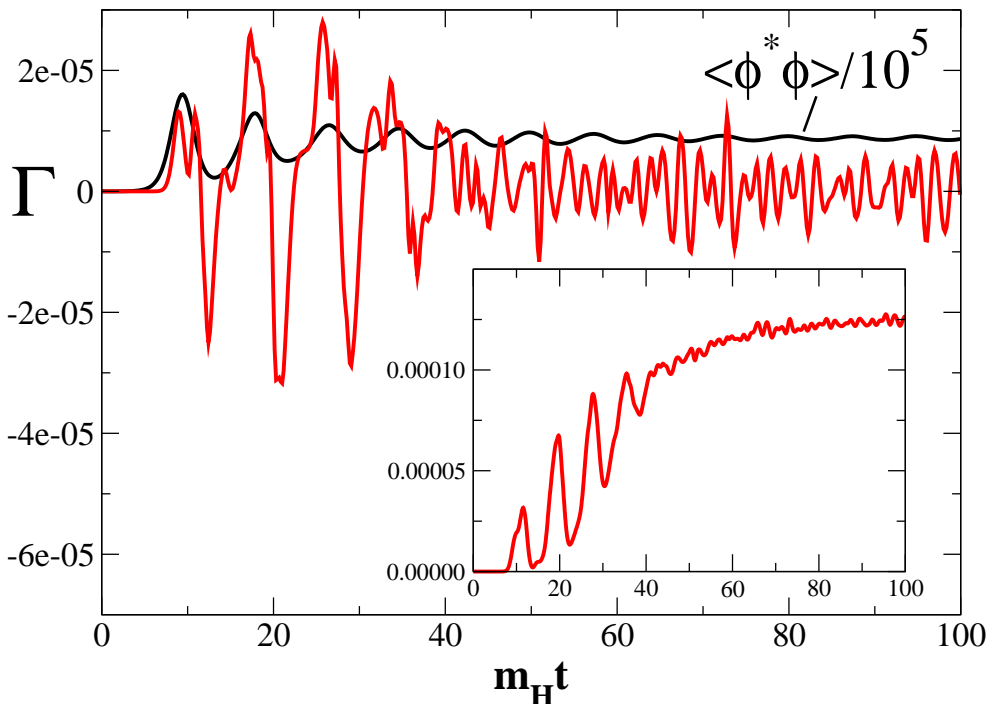


Figure 9: The effective sphaleron rate $\Gamma_{\text{eff}}/m_H^4$; $m_H/m_W = 1$, $k = 0$, Thermal initial conditions. Inset: integrated rate $\int_0^t dt' \Gamma_{\text{eff}}(t')/m_H^3$.

In the tachyonic transition such a diffusion regime is preceded by a period of preheating, where the gauge fields acquire energy and as a result a non-zero $\langle N_{\text{CS}}^2 \rangle$. The early-time rate at which this happens does not have anything to do with the equilibrium sphaleron rate. Rather, it is determined by the time scale of the preheating mechanism. Note how this rate is initially in phase with the Higgs field, but it has a large magnitude for small *and large* values of $\langle \phi^\dagger \phi \rangle$. At these early times the system is not experiencing potential barriers proportional to $\langle \phi^\dagger \phi \rangle$, with sphalerons mediating Chern-Simons number change. Even at the latest time the rate is not as small as the temperature would suggest. Averaging out the oscillations in the region $10 \lesssim tm_H \lesssim 40$, the effective slope (rate) is about $\Gamma_{\text{eff}}/m_H^4 \approx 0.35 \times 10^{-5}$, about the same value as obtained in [16]. By (5.24) this leads to the estimate (for $m_H = m_W$)

$$n_B/m_W^3 \approx 0.1 \times 10^{-5} k, \quad (5.26)$$

an order of magnitude smaller than our result (5.8) (which should be multiplied by 3 to get n_B/m_W^3).

6. Conclusion

Using numerical simulations that include effective CP violation we have obtained results for the Chern-Simons asymmetry as a function of CP-violating parameter κ . This can now be used to estimate the value of κ needed to reproduce the observed baryon asymmetry

n_B/n_γ . Following the usual arguments, this ratio is related to n_B/s , which is approximately conserved in time, where s is the entropy density. After BBN, $s = 7.04 n_\gamma$ [40], whereas after the tachyonic electroweak transition it is given by $s = (2\pi^2/45) g_* T^3$, $g_* = 86.25$ the effective number of d.o.f. in quarks, leptons, gluons and photons, and $T = 4.0\sqrt{m_H(\text{GeV})}$ GeV from (5.23). We also need $m_W = 80.5$ GeV [7]. Our results (5.7,5.8) for the asymmetry ($k = 16\pi^2\kappa m_W^2$) now lead to

$$\frac{n_B}{n_\gamma} = (0.79 \pm 0.31) \times 10^{-2} \kappa m_W^2 \quad (m_H = m_W), \quad (6.1)$$

$$= (0.46 \pm 0.21) \times 10^{-2} \kappa m_W^2 \quad (m_H = \sqrt{2} m_W). \quad (6.2)$$

Given our approximations of an instantaneous quench, initial temperature zero and the neglect of damping effects from degrees of freedom left out in the simulation, we consider these upper limits on the generated baryon asymmetry¹ (the value (6.2) is probably somewhat low, cf. sect. 5.3). To reproduce the observed baryon asymmetry (1.1) for $m_H = \sqrt{2} m_W \simeq 114$ GeV, κ has to be

$$\kappa \simeq \frac{1.4 \times 10^{-7}}{m_W^2} \simeq \frac{2.2 \times 10^{-5}}{1\text{TeV}^2}, \quad (6.3)$$

which does not seem to be particularly large. Phrasing it differently, venturing the scale $M = m_W$ (cf. (1.6)), it means

$$\delta_{\text{CP}} \simeq 0.7 \times 10^{-5}, \quad (6.4)$$

which is smaller than the Standard Model $J \simeq 3 \times 10^{-5}$ (cf. (1.4)). We see this as encouragement for further pursuing scenarios for ESM electroweak baryogenesis.

Acknowledgments

We thank Jelper Striet, Alejandro Arrizabalaga, Jon-Ivar Skullerud, Bartjan van Tent and Leo van den Horn for useful discussions. This work was supported in part by FOM/NWO. AT enjoyed support from the ESF network COSLAB.

A. Lattice formulation

This appendix contains details of the lattice formulation. The lattice spacings in the three spatial directions are $a_1 = a_2 = a_3 = a$, and in the time direction it is $a_0 \equiv a_t$ (all a_μ are positive). The parallel transporter, also called the link variable, from lattice point $x + a_\mu \hat{\mu}$ to x is² $U_{\mu,x} = U_{-\mu,x+a_\mu \hat{\mu}}^\dagger = \exp[-ia_\mu A_\mu^b(x) \tau^b/2]$, such that e.g. the forward covariant derivative on the Higgs doublet is

$$D_\mu \phi(x) = [U_{\mu,x} \phi(x + a_\mu \hat{\mu}) - \phi(x)]/a_\mu. \quad (\text{A.1})$$

¹Note, however, that we have also not taken into account the effect of CP violation *before* the transition. This may bias the initial distribution into an asymmetric form that still has zero average baryon number. See also [47, 48].

²In this appendix we use summation convention for the group indices a, b, \dots , but not for the space-time indices μ, m, n, \dots

In the following we use a re-scaled matrix form of the Higgs field defined by

$$\Phi_x = \sqrt{\lambda} a \begin{bmatrix} \phi_2^*(x) & \phi_1(x) \\ -\phi_1^*(x) & \phi_2(x) \end{bmatrix}, \quad \frac{1}{2} \text{Tr} [\Phi^\dagger \Phi] = \lambda a^2 \phi^\dagger \phi. \quad (\text{A.2})$$

Furthermore, we shall use lattice units for x and the covariant derivatives, e.g.

$$D_\mu \Phi_x = U_{\mu,x} \Phi_{x+\hat{\mu}} - \Phi_x. \quad (\text{A.3})$$

The backward covariant derivative (indicated with a prime) reads

$$D'_\mu \Phi_x = \Phi_x - U_{\mu,x-\hat{\mu}}^\dagger \Phi_{x-\hat{\mu}} = \Phi_x - U_{-\mu,x} \Phi_{x-\hat{\mu}}. \quad (\text{A.4})$$

A.1 Action

We discretize the action on a space-time lattice of size $L^3 t = (Na)^3 \times N_t a_t$ with $a_t/a \ll 1$ in the following way [35]:

$$\begin{aligned} S_L = & \sum_x \left[\beta_G^t \sum_n \left(1 - \frac{1}{2} \text{Tr} [U_{0n,x}] \right) - \beta_G^s \sum_{n>m} \left(1 - \frac{1}{2} \text{Tr} [U_{mn,x}] \right) \right. \\ & + \beta_H^t \frac{1}{2} \text{Tr} (D_0 \Phi_x)^\dagger (D_0 \Phi_x) - \beta_H^s \sum_n \frac{1}{2} \text{Tr} (D_n \Phi_x)^\dagger (D_n \Phi_x) \\ & \left. - \beta_R \left(\frac{1}{2} \text{Tr} [\Phi_x^\dagger \Phi_x] - v_{\text{lat}}^2 \right)^2 - \beta_\kappa \frac{1}{2} \text{Tr} [\Phi_x^\dagger \Phi_x] \text{Tr} [F\tilde{F}]_{\text{lat},x} \right], \quad (\text{A.5}) \end{aligned}$$

where $U_{0n,x}$ and $U_{mn,x}$ are timelike and spacelike plaquette fields defined as

$$U_{\mu\nu,x} = U_{\nu\mu,x}^\dagger = U_{\mu,x} U_{\nu,x+\hat{\mu}} U_{\mu,x+\hat{\nu}}^\dagger U_{\nu,x}^\dagger. \quad (\text{A.6})$$

The CP-violating term contains

$$\text{Tr} [F\tilde{F}]_{\text{lat},x} = - \sum_{\mu\nu\sigma\rho} \epsilon^{\mu\nu\sigma\rho} \frac{1}{2} \text{Tr} [\bar{U}_{\mu\nu,x} \bar{U}_{\sigma\rho,x}], \quad (\text{A.7})$$

where $\bar{U}_{\mu\nu,x}$ is a symmetrized plaquette field:

$$\bar{U}_{\mu\nu,x} = \frac{1}{4} (U_{\mu\nu,x} + U_{-\mu-\nu,x} + U_{-\nu\mu,x} + U_{\nu-\mu,x}). \quad (\text{A.8})$$

Matching continuum and lattice parameters we find:

$$\beta_G^t = \frac{4}{g^2} \frac{a}{a_t}, \quad \beta_G^s = \frac{4}{g^2} \frac{a_t}{a}, \quad \beta_H^t = \frac{1}{\lambda} \frac{a}{a_t}, \quad \beta_H^s = \frac{1}{\lambda} \frac{a_t}{a}, \quad (\text{A.9})$$

$$\beta_R = \frac{1}{\lambda} \frac{a_t}{a}, \quad \beta_\kappa = \frac{\kappa}{a^2 \lambda}, \quad v_{\text{lat}}^2 = \frac{(am_H)^2}{4}. \quad (\text{A.10})$$

A.2 Equations of motion

Varying the action with respect to $A_{\mu,x}^a$ gives the classical equations of motion:

$$\begin{aligned} \partial'_0 \partial_0 \Phi_x &= \frac{\beta_H^s}{\beta_H^t} \sum_n D'_n D_n \Phi_x - \frac{2\beta_R}{\beta_H^t} \left(\frac{1}{2} \text{Tr} [\Phi_x^\dagger \Phi_x] - \frac{a^2 m_H^2}{4} \right) \Phi_x \\ &\quad + \frac{2\beta_\kappa}{\beta_H^t} \text{Tr} [F\tilde{F}]_{\text{lat},x} \Phi_x, \end{aligned} \quad (\text{A.11})$$

$$\begin{aligned} -\partial'_0 E_{n,x}^a &= \frac{\beta_G^s}{\beta_G^t} \sum_m D_m'^{ab} \text{Tr} [i\tau^b U_{mn,x}] + \frac{2\beta_H^s}{\beta_G^t} \text{Tr} [(D_n \Phi_x)^\dagger i\tau^a \Phi_x] \\ &\quad + \frac{2\beta_\kappa}{\beta_G^t} \sum_{kl} \epsilon_{nkl} \left\{ \partial'_0 \left(\text{Tr} [i\tau^a U_n U_{-l-k,x+\hat{n}+\hat{0}} U_{n,x+\hat{0}}^\dagger] \text{Tr} [\Phi_{x+\hat{n}+\hat{0}}^\dagger \Phi_{x+\hat{n}+\hat{0}}] \right) \right. \\ &\quad + D_l'^{ab} \left(\text{Tr} [i\tau^b (U_{n,x} U_{l,x+\hat{n}} + U_{l,x} U_{n,x+\hat{l}}) U_{-k-0,x+\hat{n}+\hat{l}} (U_{n,x+\hat{l}}^\dagger U_{l,x}^\dagger + U_{k,x+\hat{n}}^\dagger U_{n,x}^\dagger)] \right. \\ &\quad \left. \left. \times \text{Tr} [\Phi_{x+\hat{n}+\hat{l}}^\dagger \Phi_{x+\hat{n}+\hat{l}}] \right) \right\}. \end{aligned} \quad (\text{A.12})$$

Above, we have defined the *lattice E-field* $E_{n,x}^a$ through

$$E_{n,x} = i \text{Tr} [U_{n,x} U_{n,x+\hat{0}}^\dagger \tau^a]. \quad (\text{A.13})$$

We have chosen the temporal gauge, $U_{0,x} = 0$, and $D_m'^{ab}$ is the backward covariant derivative in the adjoint representation, e.g.

$$D_m'^{ab} E_{j,x}^b = E_{j,x}^a - \frac{1}{2} \text{Tr} [U_{-m,x}^\dagger \tau^a U_{-m,x} \tau^b] E_{j,x-\hat{m}}^b. \quad (\text{A.14})$$

The variation with respect to A_0 gives the Gauss constraint:

$$\begin{aligned} 0 = C_x^a &\equiv - \sum_n D_n'^{ab} E_{x,n}^b + \frac{2\beta_H^t}{\beta_G^t} \text{Tr} [\partial_0 \Phi_x^\dagger i\tau^a \Phi_x] \\ &\quad - \frac{2\beta_\kappa}{\beta_G^t} \sum_{jkl} \epsilon_{jkl} D_j'^{ab} \left(\text{Tr} [i\tau^b U_{j,x} U_{-l-k,x+\hat{j}+\hat{0}} U_{j,x+\hat{0}}^\dagger] \text{Tr} [\Phi_{x+\hat{j}+\hat{0}}^\dagger \Phi_{x+\hat{j}+\hat{0}}] \right). \end{aligned} \quad (\text{A.15})$$

A Noether argument tells us that the quantity C_x^a is conserved in (lattice) time for each \mathbf{x} when evolving the system with the equations of motion.

Because of the symmetrization in the discretization of $\text{Tr} F\tilde{F}$, which we found to be important for reducing discretization errors, both the Higgs and the gauge field equations of motion are *implicit*. They depend in a non-linear way on forward (in time) links and Higgs fields. We solve these equations by iteration. With sufficiently small time steps and/or κ convergence should be good, and indeed we encountered no problems, iterating between 3 and 9 times per time step with $a_t/a = 0.05$. However, the computational costs were correspondingly large. We iterated to computer accuracy (double precision) and checked that the Gauss constraint is satisfied, again to computer accuracy.

A.3 Chern-Simons number and winding number

The lattice expression for the change in Chern-Simons number is given by

$$N_{\text{CS}}(t) - N_{\text{CS}}(0) = \frac{1}{16\pi^2} \sum_0^t \sum_{\mathbf{x}} \text{Tr} [F\tilde{F}]_{\text{lat},x}, \quad (\text{A.16})$$

where $\text{Tr} [F\tilde{F}]_{\text{lat},x}$ is given in (A.7). The following lattice implementation of the winding number in the Higgs field,

$$N_{\text{w}} = \frac{1}{192\pi^2} \sum_{\mathbf{x},ijk} \epsilon_{ijk} \text{Tr} \left[(V_{x+\hat{i}} - V_{x-\hat{i}}) V_x^\dagger (V_{x+\hat{j}} - V_{x-\hat{j}}) V_x^\dagger (V_{x+\hat{k}} - V_{x-\hat{k}}) V_x^\dagger \right], \quad (\text{A.17})$$

where $V_x = V(x)$ with $V(x)$ the SU(2) matrix defined in (5.5), turned out to perform satisfactorily in our simulation.

B. Coping with the Gauss constraints

B.1 Initial Higgs fields

Our task is to generate an ensemble of initial conditions for the Higgs field in our classical simulations according to the distribution (4.4,4.5,4.14). The distribution applies to a real scalar field with the definitions

$$\phi(\mathbf{x}) = \sum_{\mathbf{k}} \frac{e^{i\mathbf{k}\cdot\mathbf{x}}}{\sqrt{L^3}} \phi_{\mathbf{k}}, \quad \pi(\mathbf{x}) = \sum_{\mathbf{k}} \frac{e^{i\mathbf{k}\cdot\mathbf{x}}}{\sqrt{L^3}} \pi_{\mathbf{k}}. \quad (\text{B.1})$$

In finite volume the momentum label takes on the discrete values $\mathbf{k} = 2\pi\mathbf{n}/L$, and on the lattice with lattice spacing $a = L/N$ we can choose $n_j = -(N/2 - 1), \dots, 0, \dots, N/2$. The reality of the fields imposes $\phi_{\mathbf{k}} = \phi_{-\mathbf{k}}^\dagger$ and similarly for the canonical momenta, except for the special modes $\mathbf{n} = (0 \text{ or } N/2, 0 \text{ or } N/2, 0 \text{ or } N/2)$, for which $\exp(i\mathbf{k} \cdot \mathbf{x})$ is real, and so the reality conditions imply that the corresponding $\phi_{\mathbf{k}}$ and $\pi_{\mathbf{k}}$ are real. We shall term them ‘‘corner’’ modes. There are 8 of them. The rest we may as well name ‘‘bulk’’ modes. We can write these latter complex variables as

$$\phi_{\mathbf{k}}^\alpha = \frac{1}{\sqrt{2\omega_{\mathbf{k}}}} (a_{\mathbf{k}}^\alpha + ib_{\mathbf{k}}^\alpha), \quad \pi_{\mathbf{k}}^\alpha = \sqrt{\frac{\omega_{\mathbf{k}}}{2}} (c_{\mathbf{k}}^\alpha + id_{\mathbf{k}}^\alpha). \quad (\text{B.2})$$

We have put in a label $\alpha = 1, 2, 3, 4$ for the real fields of the Higgs field doublet:

$$\phi^T = \left(\frac{\phi^1 + i\phi^2}{\sqrt{2}}, \frac{\phi^3 + i\phi^4}{\sqrt{2}} \right), \quad (\text{B.3})$$

and similar for the canonical conjugate π . On the lattice we have

$$\omega_{\mathbf{k}} \rightarrow \sqrt{\mu^2 + \mathbf{k}_{\text{lat}}^2}, \quad \mathbf{k}_{\text{lat}}^2 = \sum_j (2 - 2\cos(k_j a)) / a^2, \quad (\text{B.4})$$

and the lattice Higgs doublet is defined as

$$\phi_{\mathbf{x}} = a\phi(x). \quad (\text{B.5})$$

We continue to use lattice units and define the lattice canonical conjugate of $\phi_{\mathbf{x}}$ as

$$\pi_{\mathbf{x}} = \partial_0 \phi_{\mathbf{x}} = \phi_{\mathbf{x}+\hat{0}} - \phi_{\mathbf{x}}. \quad (\text{B.6})$$

For the corner modes, the $b_{\mathbf{k}}^\alpha$ and $d_{\mathbf{k}}^\alpha$ are just zero.

For each spatial lattice site there are three Gauss constraints (one for each generator of the gauge group) to be satisfied by the initial configurations. In terms of³

$$\rho_{\mathbf{x}}^\alpha = ig^2 \frac{1}{2} \left(\pi^\dagger \tau^\alpha \phi - \phi^\dagger \tau^\alpha \pi \right)_{\mathbf{x}} = i \frac{2\beta_H^t}{\beta_G^t} \text{Tr} [\partial_0 \Phi^\dagger \tau^\alpha \Phi]_{\mathbf{x}}, \quad \alpha = 1, \dots, 4, \quad (\text{B.7})$$

the constraints read

$$\partial'_n E_{n,\mathbf{x}}^a = \rho_{\mathbf{x}}^a, \quad (\text{B.8})$$

where we have used the fact that our initial $A_n^a = 0$. Integrating the left and right hand sides in a periodic volume, this reduces to three global Gauss constraints,

$$0 = \sum_{\mathbf{x}} \rho_{\mathbf{x}}^\beta, \quad \beta = 1, 2, 3. \quad (\text{B.9})$$

These are three constraints on our many Fourier modes. Because we have four real scalar fields it is convenient to impose an additional fourth constraint:

$$0 = \sum_{\mathbf{x}} \rho_{\mathbf{x}}^\beta, \quad \beta = 4, \quad (\text{B.10})$$

which can be seen as the requirement that the total hypercharge also vanishes in the periodic volume. Since it is only one extra global constraint on the many modes we do not expect that imposing it or not has a noticeable effect on the physical results.

Inserting equations (B.1), (B.2) and (B.3) into (B.9) and (B.10) we get a set of constraints on the $a_{\mathbf{k}}, b_{\mathbf{k}}, c_{\mathbf{k}}, d_{\mathbf{k}}$, of which the last one ($\beta = 4$) is

$$0 = \sum_{\alpha} \left[\sum_{\mathbf{k}_{\text{corner}}} (c_{\mathbf{k}}^\alpha a_{\mathbf{k}}^\alpha) + \sum_{\mathbf{k}_{\text{bulk}}} 2 (c_{\mathbf{k}}^\alpha a_{\mathbf{k}}^\alpha + d_{\mathbf{k}}^\alpha b_{\mathbf{k}}^\alpha) \right] = \sum_{\alpha} [c_{\mathbf{0}}^\alpha a_{\mathbf{0}}^\alpha] + f_4, \quad (\text{B.11})$$

where we have singled out the $\mathbf{k} = (0, 0, 0)$ component for later use, and dumped the rest into the quantity f_4 . In a similar way it is easy to find for the constraints for $\beta = 1, 2, 3$:

$$0 = c_{\mathbf{0}}^2 a_{\mathbf{0}}^3 - c_{\mathbf{0}}^3 a_{\mathbf{0}}^2 + c_{\mathbf{0}}^4 a_{\mathbf{0}}^1 - c_{\mathbf{0}}^1 a_{\mathbf{0}}^4 + f_1, \quad (\text{B.12})$$

$$0 = c_{\mathbf{0}}^1 a_{\mathbf{0}}^3 - c_{\mathbf{0}}^3 a_{\mathbf{0}}^1 + c_{\mathbf{0}}^2 a_{\mathbf{0}}^4 - c_{\mathbf{0}}^4 a_{\mathbf{0}}^2 + f_2, \quad (\text{B.13})$$

$$0 = c_{\mathbf{0}}^2 a_{\mathbf{0}}^1 - c_{\mathbf{0}}^1 a_{\mathbf{0}}^2 + c_{\mathbf{0}}^3 a_{\mathbf{0}}^4 - c_{\mathbf{0}}^4 a_{\mathbf{0}}^3 + f_3, \quad (\text{B.14})$$

where again $f_{1,2,3}$ are straightforward but long combinations of the remaining variables.

These equations are linear in all the variables and can be written as

$$\mathbf{0} = \mathbf{M} \mathbf{c}_0 + \mathbf{f}, \quad (\text{B.15})$$

³We denote the 2×2 unit matrix by τ^4 .

with $\mathbf{M} = \mathbf{M}(\mathbf{a}_0)$ a 4 by 4 matrix. We are left with the task of generating sets of random numbers according to the distribution

$$P(a, b, c, d) \propto \exp \left(-\frac{1}{2} \sum_{\mathbf{k}, \alpha} \frac{a_{\mathbf{k}}^{\alpha 2} + b_{\mathbf{k}}^{\alpha 2} + c_{\mathbf{k}}^{\alpha 2} + d_{\mathbf{k}}^{\alpha 2}}{n_{\mathbf{k}} + 1/2} \right) \delta(\mathbf{M}\mathbf{c}_0 + \mathbf{f}). \quad (\text{B.16})$$

We can integrate out the c_0^α to get

$$P(a, b, c, d) \propto \frac{1}{\det \mathbf{M}} \exp \left(-\frac{1}{2} \sum'_{\mathbf{k}, \alpha} \frac{a_{\mathbf{k}}^{\alpha 2} + b_{\mathbf{k}}^{\alpha 2} + c_{\mathbf{k}}^{\alpha 2} + d_{\mathbf{k}}^{\alpha 2}}{n_{\mathbf{k}} + 1/2} - \frac{1}{2} \frac{\mathbf{G}^2}{n_0 + 1/2} \right), \quad (\text{B.17})$$

where the prime indicates that the sum over modes no longer includes the c_0^α , and

$$\mathbf{G}^2 = (\mathbf{M}^{-1}\mathbf{f})^T \mathbf{M}^{-1}\mathbf{f} = \frac{\sum_{\alpha} f_{\alpha}^2}{\sum_{\alpha} a_0^{\alpha 2}}, \quad (\text{B.18})$$

$$\det \mathbf{M} = \sum_{\alpha} a_0^{\alpha 2}. \quad (\text{B.19})$$

The distribution is no longer a product of Gaussians and we sample it using a Monte-Carlo algorithm. For every realization of the remaining unconstrained variables, we then solve for the c_0^α , such that the global Gauss constraints are fulfilled.

Sampling a distribution with a δ -function can be difficult, and can require very elaborate Monte-Carlo algorithms. However, having sufficiently many degrees of freedom to “distribute the constraints on”, the deviation from (in this case) a Gaussian distribution is small. In our simulation, where there are about 50 unstable modes (when using Just-the-half) and the whole collection of lattice modes when using Thermal, we did not encounter such problems.

B.2 Initial gauge fields

The Gauss constraint (eqs. A.15) imposes a constraint on the gauge fields at each point in space, given a Higgs field configuration. Keeping in mind that the gauge fields only grow large and classical because of the coupling to the Higgs fields, we set the gauge fields to zero initially. This simplifies the constraints dramatically, to read:

$$0 = C_x^a = -\partial'_n E_{n,x}^a + \frac{2\beta_H^t}{\beta_G^t} \text{Tr} \left[(\partial_0 \Phi_x)^\dagger i\tau^a \Phi_x \right]. \quad (\text{B.20})$$

We put C_x^a to zero at each point in space, which means that there are no sources other than the Higgs field. Given the Higgs fields we can now write:

$$\partial'_n E_{n,\mathbf{x}}^a(x) = \rho_{\mathbf{x}}^a, \quad a = 1, 2, 3, \quad (\text{B.21})$$

which is just a Coulomb equation, and is solved by introducing a set of scalar functions $\chi_{\mathbf{x}}^a$ so that

$$E_{n,\mathbf{x}}^a = -\partial_n \chi_{\mathbf{x}}^a. \quad (\text{B.22})$$

Fourier transforming

$$-\partial_n \partial'_n \chi_{\mathbf{x}}^a = \rho_{\mathbf{x}}^a \quad (\text{B.23})$$

gives

$$\tilde{\chi}^a(\mathbf{k}) = \frac{\tilde{\rho}_{\mathbf{k}}^a}{\mathbf{k}_{\text{lat}}^2}. \quad (\text{B.24})$$

Since we use a periodic volume, $\tilde{\rho}_{\mathbf{k}}^a$ should vanish at $\mathbf{k} = 0$, i.e. the global Gauss constraints on the Higgs fields

$$0 = \sum_{\mathbf{x}} \partial'_n E_{n,\mathbf{x}}^a = \sum_{\mathbf{x}} \rho_{\mathbf{x}}^a \quad (\text{B.25})$$

have to be satisfied. Their implementation is described in the previous section.

References

- [1] D. N. Spergel *et. al.*, *First year Wilkinson Microwave Anisotropy Probe (WMAP) observations: Determination of cosmological parameters*, *Astrophys. J. Suppl.* **148** (2003) 175, [[astro-ph/0302209](#)].
- [2] A. D. Sakharov, *Violation of CP invariance, C asymmetry, and baryon asymmetry of the universe*, *Pisma Zh. Eksp. Teor. Fiz.* **5** (1967) 32–35.
- [3] M. Dine and A. Kusenko, *The origin of the matter-antimatter asymmetry*, [hep-ph/0303065](#).
- [4] G. 't Hooft, *Symmetry breaking through Bell-Jackiw anomalies*, *Phys. Rev. Lett.* **37** (1976) 8–11.
- [5] N. Cabibbo, *Unitary symmetry and leptonic decays*, *Phys. Rev. Lett.* **10** (1963) 531–532.
- [6] M. Kobayashi and T. Maskawa, *CP violation in the renormalizable theory of weak interaction*, *Prog. Theor. Phys.* **49** (1973) 652–657.
- [7] **Particle Data Group** Collaboration, K. Hagiwara *et. al.*, *Review of particle physics*, *Phys. Rev.* **D66** (2002) 010001.
- [8] W. Buchmuller, P. Di Bari, and M. Plumacher, *The neutrino mass window for baryogenesis*, *Nucl. Phys.* **B665** (2003) 445–468, [[hep-ph/0302092](#)].
- [9] V. A. Kuzmin, V. A. Rubakov, and M. E. Shaposhnikov, *On the anomalous electroweak baryon number nonconservation in the early universe*, *Phys. Lett.* **B155** (1985) 36.
- [10] V. A. Rubakov and M. E. Shaposhnikov, *Electroweak baryon number non-conservation in the early universe and in high-energy collisions*, *Usp. Fiz. Nauk* **166** (1996) 493–537, [[hep-ph/9603208](#)].
- [11] A. G. Cohen, D. B. Kaplan, and A. E. Nelson, *Progress in electroweak baryogenesis*, *Ann. Rev. Nucl. Part. Sci.* **43** (1993) 27–70, [[hep-ph/9302210](#)].
- [12] K. Kajantie, M. Laine, K. Rummukainen, and M. E. Shaposhnikov, *The electroweak phase transition: A non-perturbative analysis*, *Nucl. Phys.* **B466** (1996) 189–258, [[hep-lat/9510020](#)].
- [13] F. Csikor, Z. Fodor, and J. Heitger, *Endpoint of the hot electroweak phase transition*, *Phys. Rev. Lett.* **82** (1999) 21–24, [[hep-ph/9809291](#)].

- [14] M. Carena, M. Quiros, and C. E. M. Wagner, *Opening the window for electroweak baryogenesis*, *Phys. Lett.* **B380** (1996) 81–91, [[hep-ph/9603420](#)].
- [15] M. Laine and K. Rummukainen, *The MSSM electroweak phase transition on the lattice*, *Nucl. Phys.* **B535** (1998) 423–457, [[hep-lat/9804019](#)].
- [16] J. Garcia-Bellido, D. Y. Grigoriev, A. Kusenko, and M. E. Shaposhnikov, *Non-equilibrium electroweak baryogenesis from preheating after inflation*, *Phys. Rev.* **D60** (1999) 123504, [[hep-ph/9902449](#)].
- [17] L. M. Krauss and M. Trodden, *Baryogenesis below the electroweak scale*, *Phys. Rev. Lett.* **83** (1999) 1502–1505, [[hep-ph/9902420](#)].
- [18] E. J. Copeland, D. Lyth, A. Rajantie, and M. Trodden, *Hybrid inflation and baryogenesis at the TeV scale*, *Phys. Rev.* **D64** (2001) 043506, [[hep-ph/0103231](#)].
- [19] A. Rajantie, P. M. Saffin, and E. J. Copeland, *Electroweak preheating on a lattice*, *Phys. Rev.* **D63** (2001) 123512, [[hep-ph/0012097](#)].
- [20] E. J. Copeland, S. Pascoli, and A. Rajantie, *Dynamics of tachyonic preheating after hybrid inflation*, *Phys. Rev.* **D65** (2002) 103517, [[hep-ph/0202031](#)].
- [21] J. Garcia-Bellido, M. Garcia Perez, and A. Gonzalez-Arroyo, *Symmetry breaking and false vacuum decay after hybrid inflation*, *Phys. Rev.* **D67** (2003) 103501, [[hep-ph/0208228](#)].
- [22] J. Smit and A. Tranberg, *Chern-Simons number asymmetry from CP violation at electroweak tachyonic preheating*, *JHEP* **12** (2002) 020, [[hep-ph/0211243](#)].
- [23] J. García-Bellido, M. Garcia-Perez, and A. Gonzalez-Arroyo, *Chern-Simons production during preheating in hybrid inflation models*, [hep-ph/0304285](#).
- [24] C. Jarlskog, *Commutator of the quark mass matrices in the standard electroweak model and a measure of maximal CP violation*, *Phys. Rev. Lett.* **55** (1985) 1039.
- [25] M. E. Shaposhnikov, *Baryon asymmetry of the universe in standard electroweak theory*, *Nucl. Phys.* **B287** (1987) 757–775.
- [26] M. E. Shaposhnikov, *Structure of the high temperature gauge ground state and electroweak production of the baryon asymmetry*, *Nucl. Phys.* **B299** (1988) 797.
- [27] G. R. Farrar and M. E. Shaposhnikov, *Baryon asymmetry of the universe in the minimal Standard Model*, *Phys. Rev. Lett.* **70** (1993) 2833–2836, [[hep-ph/9305274](#)]. [[Erratum-ibid.71:210,1993](#)].
- [28] G. R. Farrar and M. E. Shaposhnikov, *Baryon asymmetry of the universe in the standard electroweak theory*, *Phys. Rev.* **D50** (1994) 774, [[hep-ph/9305275](#)]. [[Erratum-ibid.71:210,1993](#)].
- [29] G. R. Farrar and M. E. Shaposhnikov, *Note added to 'Baryon asymmetry of the universe in the standard model'*, [hep-ph/9406387](#).
- [30] T. Konstandin, T. Prokopec, and M. G. Schmidt, *Axial currents from CKM matrix CP violation and electroweak baryogenesis*, [hep-ph/0309291](#).
- [31] J. Smit, “Tachyonic electroweak transition, CP violation and baryogenesis.” Talk at Cosmo-03, Ambleside, UK.
- [32] D. Bodeker, G. D. Moore, and K. Rummukainen, *Chern-Simons number diffusion and hard thermal loops on the lattice*, *Phys. Rev.* **D61** (2000) 056003, [[hep-ph/9907545](#)].

- [33] G. D. Moore, *Measuring the broken phase sphaleron rate nonperturbatively*, *Phys. Rev.* **D59** (1999) 014503, [[hep-ph/9805264](#)].
- [34] J.-I. Skullerud, J. Smit, and A. Tranberg, *W and Higgs particle distributions during electroweak tachyonic preheating*, *JHEP* **08** (2003) 045, [[hep-ph/0307094](#)].
- [35] J. Ambjorn, T. Askgaard, H. Porter, and M. E. Shaposhnikov, *Sphaleron transitions and baryon asymmetry: A numerical real time analysis*, *Nucl. Phys.* **B353** (1991) 346–378.
- [36] D. Y. Grigoriev, M. E. Shaposhnikov, and N. Turok, *Electroweak baryogenesis: A numerical study in (1+1)- dimensions*, *Phys. Lett.* **B275** (1992) 395–402.
- [37] J. Smit and A. Tranberg, *Chern-Simons number asymmetry from CP-violation during tachyonic preheating*, in *Strong and Electroweak Matter 2002 – Proceedings of the SEWM2002 Meeting* (M. G. Schmidt, ed.), (Singapore), World Scientific, 2002. <http://arXiv.org/abs/hep-ph/0210348>.
- [38] J. Smit and A. Tranberg, *Classical issues in electroweak baryogenesis*, [hep-lat/0309082](#).
- [39] A. Tranberg, “Baryogenesis from CP violation at electroweak tachyonic preheating.” Talk at Cosmo-03, Ambleside, UK.
- [40] E. W. Kolb and M. S. Turner, *The Early Universe*. Addison-Wesley, Reading, Massachusetts, 1990.
- [41] P. J. E. Peebles and A. Vilenkin, *Quintessential inflation*, *Phys. Rev.* **D59** (1999) 063505, [[astro-ph/9810509](#)].
- [42] G. German, G. Ross, and S. Sarkar, *Low-scale inflation*, *Nucl. Phys.* **B608** (2001) 423–450, [[hep-ph/0103243](#)].
- [43] A. Berera and R. O. Ramos, *Absence of isentropic expansion in various inflation models*, [hep-ph/0308211](#).
- [44] T. Asaka, W. Buchmuller, and L. Covi, *False vacuum decay after inflation*, *Phys. Lett.* **B510** (2001) 271–276, [[hep-ph/0104037](#)].
- [45] G. N. Felder *et. al.*, *Dynamics of symmetry breaking and tachyonic preheating*, *Phys. Rev. Lett.* **87** (2001) 011601, [[hep-ph/0012142](#)].
- [46] J. Smit, J. C. Vink, and M. Salle, *Initial conditions for simulated ‘tachyonic preheating’ and the Hartree ensemble approximation*, [hep-ph/0112057](#). Contribution to Cosmo-01, Rovaniemi, Finland.
- [47] B.-J. Nauta and A. Arrizabalaga, *Asymmetric Chern-Simons number diffusion from CP-violation*, *Nucl. Phys.* **B635** (2002) 255–285, [[hep-ph/0202115](#)].
- [48] B.-J. Nauta, *On asymmetric Chern-Simons number diffusion*, in *Strong and Electroweak Matter 2002 – Proceedings of the SEWM2002 Meeting* (M. G. Schmidt, ed.), (Singapore), World Scientific, 2002. <http://arXiv.org/abs/hep-ph/0301150>.